

A method for myocardial contraction force reconstruction for tissue viability assessment

Cristian A. Linte^{1,3}, Terry M. Peters^{1,2,3} and Abbas Samani^{1,2,3}

¹Biomedical Engineering Graduate Program, University of Western Ontario,
London, ON, Canada, N6A 5B9

²Department of Medical Biophysics, University of Western Ontario,
London, ON, Canada, N6A 5C1

³Imaging Research Laboratories, Robarts Research Institute, London, ON, Canada, N6A 5K8

ABSTRACT

Myocardial infarction results in myocardial necrosis, usually caused by an imbalance in the oxygen supply and demand to myocardial tissue. To our knowledge there is no technique that can provide quantitative direct information concerning the intensity, extent and location of the infarction. Contraction forces generated by cardiac tissues represent a quantitative and direct measure of the myocardial functionality, since it is expected that infarcted tissue generate little or no contraction force. Our objective is to develop a biomechanics based reconstruction technique to image myocardial contraction forces, for the purpose of assessing the viability of cardiac tissues. This technique is designed to reconstruct the contraction forces by inverting myocardial tissue displacement data acquired throughout heart beat cycles using conventional imaging techniques. Recognizing that myocardial contraction force distribution is 3D, we assumed an axisymmetric myocardial geometry to demonstrate the concept. With this assumption, the inversion algorithm was developed and implemented in 2D space. As a preliminary analysis, a simulation involving a 2D representation of myocardial wall tissue was carried out. The tissue was modeled as a homogeneous material with isotropic and linear elastic material properties. Assuming an axisymmetric contraction force distribution, a finite element analysis was performed on the tissue model, and a 2D displacement field was generated. The developed inversion algorithm was then employed to reconstruct the force distribution, which was ultimately compared to the original force field. The reconstruction error, estimated as the difference between the two force fields and normalized by the magnitude of the reference distribution, averaged to $\pm 10\%$. Results demonstrate that our myocardial contraction force reconstruction algorithm is reasonably accurate and robust.

Keywords: Myocardium, infarction, contraction force, inversion technique, medical imaging modalities

1. INTRODUCTION

Cardiovascular diseases have caused 16.7 million deaths per year worldwide according to the 2002 monitoring report of the World Health Organization, and this number is expected to rise above 20 million per year in 2010. They cause half of all deaths in many developed countries and account for one of the main causes of death in developing countries. One of the most threatening conditions is cardiac ischemia, also known as angina pectoris, which leads to myocardial infarction (MI). MI results in myocardial necrosis, usually due to an imbalance of oxygen supply and demand, caused by the blockage of an artery responsible for irrigating a particular region of the heart muscle with blood. In 98% of the cases it occurs as a result of the process of atherosclerosis (i.e. hardening of arteries) in the coronary vessels. Clinical complications of MI depend on the intensity, size and location of the infarction, as well as the pre-existing damage. To our knowledge, there is no quantitative non-invasive technique that can reliably provide the location of necrosis, and assess the extent and intensity of tissue damage due to infarction. If detected early and accurately, this information would be crucial for clinicians to determine the appropriate course of therapy that minimizes further complications and reduces the period of hospitalization and health care cost.

Previous minimally invasive techniques for diagnosis of MI have been developed based on various medical imaging modalities. More recently a different approach for myocardial tissue viability assessment has emerged. This approach is based on analyzing myocardial tissue deformation measured using ultrasound (US) or magnetic resonance

imaging (MRI) throughout the cardiac cycle. It is now possible to study regional myocardial deformation in the clinical setting by calculating its velocity data using cardiac US^{1,2,3} or (MRI)^{3,4}. While the latter provides velocity information at a reasonable spatial resolution, the frame rate is not sufficiently high for accurate temporal analysis⁵. In contrast, Doppler US imaging can provide real-time regional velocity information at 150 frames/s with high axial and sufficient lateral resolution in a two dimensional format^{6,7}. The US images were acquired and it was determined that normally contracting myocardial segments can be distinguished from segments belonging to chronically infarcted zones using strain imaging techniques, by analyzing the time pattern for myocardial shortening and lengthening or the systolic peak strain rate measurements⁸. MRI has been frequently employed in assessing the viability of cardiac tissue, since it can provide a three dimensional analysis of global and regional cardiac function with great accuracy and reproducibility⁹. An important clinical application of regional functional analysis is the assessment of reversibility of injured, yet viable myocardium in ischemic heart disease^{10,11}. Left ventricular remodeling is a phenomenon which begins with the onset of the infarction, resulting in expansion associated with wall thinning in the diseased area, while the healthy zone will hypertrophy and dilate. The remodeling intensity is a function of both physiological and mechanical factors, depending on the size and localization of the infarction, as well as the afterload, evaluated by means of the end-systolic wall stress¹². The end-systolic wall stress is estimated from the left ventricular systolic pressure and a geometric factor dependant on the shape of the ventricle¹³. Because of good spatial resolution and an absence of geometric hypothesis, MRI allows for a precise definition of the epicardial and endocardial surfaces of the left ventricle, and for an accurate identification of the myocardial deformation in infarction during the cardiac cycle^{14,15,9}. While wall thickening accounts for myocardial deformation in the radial direction only, strain imaging methods allow for the measurement of all components of myocardial contraction at once¹⁶. Strain imaging involves the assessment of local tissue deformation as an indicator of myocardial contractile function¹⁷. A method coupled with strain imaging techniques used in interpreting collected strain measurements involves the computation of the shortening index, an overall non-dimensional measure of tissue deformation in all three directions of the space¹⁸. Although a quantifiable parameter, the shortening index is only capable of providing the clinician with a qualitative measure of the cardiac deformations, and it is highly subjective. Its interpretation requires a shortening index database of healthy people and previously diagnosed patients. Such a database is necessary for an assessment based on a relative comparison by the clinician.

Since the quantitative assessment of the deformation pattern has proved to be useful in the diagnosis of myocardial ischemia and cardiac infarction, the use of the newly developed technique of magnetic resonance (MR) tagging was a break-through in the kinematic analysis of the heart^{19,20,21}. MR tagging uses the technique of spatial modulation of the magnetization to quantitatively determine the motion of a grid of tags attached to the cardiac tissue non-invasively²².

The specific aim of our work is to investigate the possibility of developing a biomechanical-based assessment method capable of assisting in quantifying the extent and intensity of myocardial damage due to infarction. Contraction forces generated by myocardial tissues are indicative of their viability, and thus can be regarded as a quantitative, direct measure of the myocardium functionality. As one would expect, damaged tissue, such as the tissue regions affected by infarction, would generate little or no contraction force. As such, an imaging technique that visualizes the myocardial contraction force distribution would be a valuable tool for diagnosis. Based on the anatomical structure of the cardiac tissue, the left ventricular myocardium contains a high density of muscle fibers, each capable of outputting relatively mild local contractions, but globally amplified through a cascade effect achieved by engaging a large ensemble of myofibrils²³. Therefore, the heart muscle can be modeled as a deformable solid, which can generate an internal force distributed throughout its entire volume. In this model, we assume that the displacements within the ventricular walls are solely generated by the contraction forces. In this article we describe an algorithm for myocardial contraction force reconstruction, and present preliminary results based on simulated myocardial tissue deformation.

2. METHOD

This technique is based on soft tissue biomechanics, which relies on the cardiac tissue capability to generate contraction forces in response to an electric stimulus. Accordingly, we model the myocardium as a deformable solid, which can generate an internal contraction force distributed throughout its mass. This method assumes that the heart has reached its steady-state operating conditions, with no external factors contributing to irregularities in the cardiac cycle. Although the myocardial tissue is highly non-linear and anisotropic²³, we initially model it as a linear, elastic, isotropic and nearly incompressible continuum, an assumption used frequently for modeling a large variety of biological tissues. This proposed contraction force reconstruction technique is based on a typical inverse problem formulation that consists

of two main components: a finite element (FE) deformable cardiac model, which represents the direct problem model, and an inversion algorithm.

2.1.1 Deformable myocardial model

The deformable model must be capable of simulating myocardial deformations throughout the cardiac cycle. Its geometry can be extracted by segmentation of high quality medical images acquired through MRI or computed tomography (CT). These images allow for a reasonably accurate definition of the epicardial and endocardial borders of the myocardium, given their high contrast and spatial resolution¹².

2.1.2 Myocardial displacement field acquisition

Myocardial displacement data can be acquired throughout the cardiac cycle using special medical imaging techniques such as MRI tagging, where the entire image space is tagged with a particular spatially encoded pattern which conforms to the geometry of the heart muscle and deforms with the tissue, providing virtual markers that reflect the local displacement of the myocardium²⁴. These displacement images are processed on a slice-by-slice basis, and the results assembled into a three-dimensional displacement field of user-defined resolution.

2.1.3 Force reconstruction algorithm

The core component of this technique is the inversion algorithm, which is based on continuum mechanics principles applied to soft tissue deformation. Continuum mechanics leads to equation (1), which is a variation of the Navier equation, in which the contraction forces are modeled as body forces:

$$\frac{E}{2(1+\nu)} \Delta u + \frac{E}{2(1+\nu)(1-2\nu)} \nabla \nabla u + \rho \cdot f = \rho \cdot \partial_t^2 u \quad (1)$$

where E is the tissue Young's modulus, u is the displacement field, f is the body force (per unit mass of material), ρ is the tissue density and ν is its Poisson's ratio. The purpose of this algorithm is to solve for the body force component f in the equation, by inverting the measured myocardial tissue displacements u . The inversion algorithm uses the FE cardiac model as a computational domain, the 3D myocardial displacement field constitutes its input, and the contraction force distribution represents the output. One limitation of the Navier equation is that it assumes linear elastic and isotropic material.

2.2 Two-dimensional (2D) analysis of a thin myocardial slice

2.2.1 Direct problem – thin slice modeling

To illustrate the concepts described above, the 3D analysis was simplified to a 2D problem assuming an axisymmetric geometry and force distribution in the myocardium. In this manner a 2D representation of myocardial tissue was simulated using finite elements. The shape of the tissue geometry is shown in Figure 1, which is based on the anatomical left ventricular geometry of a canine heart, previously explored in the literature²⁵. Since this demonstration is based on simulated data, a direct problem was first formulated in order to generate a set of displacement data, by building an axisymmetric FE model of the tissue using commercial software (ABAQUS 6.4). The output of the FE analysis consisting of nodal displacements was used as input for the inversion algorithm, which will be described in detail in a later section. Mechanical properties of the tissue were carefully chosen to mimic linear, elastic and nearly incompressible behaviour of myocardial tissue at maximum deformation state, with a Young's modulus of 30 kPa and a Poisson's ratio of 0.495²⁵. The geometry of the myocardium was discretized using a custom developed FE meshing algorithm that led to a mesh of isotropic pixels of 1 mm x 1 mm in size. This mesh was selected to be consistent with the inverse problem computations in which the finite difference method was used to approximate spatial derivatives in equation (1).

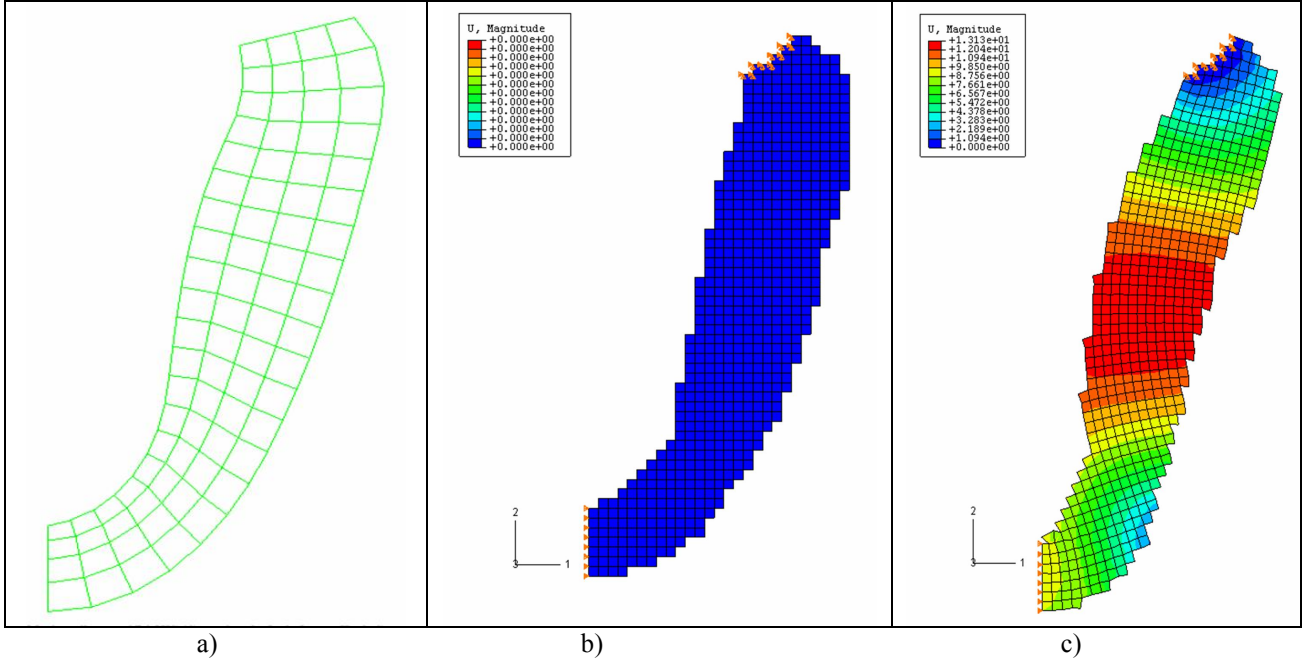


Figure 1: a) Canine left ventricular geometry used for myocardial tissue simulation; b) Undeformed shape of the discretized cardiac tissue slice; c) Deformed shape of the tissue slice under the effect of distributed body force loading

2.2.2 Boundary conditions

The 2D model consists of four distinct borders: apical, basal, epicardial and endocardial. Each of these margins was assigned boundary conditions according to the physiology of the myocardium. The apical boundary was constrained to only slide along the vertical direction since the myocardium elongates towards the apex during the cardiac cycle. The basal boundary was situated adjacent to the mitral valve and we assumed that there was no significant contraction at this particular area. As such the basal boundary was constrained from any translations. The epicardial and endocardial boundaries were modeled as free edges.

2.2.3 Loading conditions

Following the anatomy and physiology of the myocardium, and making use of classical principles of continuum mechanics, we assumed that the myocardium contraction results from an internal force distributed across the volume of the tissue. This contraction was represented by the body force (f) term in the Navier equation. In order to simulate the systolic and diastolic phases, we used harmonic force functions, with driving frequencies expressed as scalar multiples of the steady state heart rate of 60 beats per minute (1.2 Hz). Assuming linear behavior, the harmonic myocardial contractions were obtained by superimposing the effects of each sinusoidal force component.

2.2.4 Inverse problem – contraction force reconstruction

The inverse problem was formulated for the myocardial contraction force reconstruction, using an algorithm that solves for the body forces in the Navier partial differential equations of linear elasticity. Equation (2) is the Navier equation expressed in the Cartesian coordinates of the myocardial slice plane. Using this algorithm, the contraction forces may be reconstructed by inverting the measured tissue displacements acquired through heart cardiac cycle.

$$\begin{aligned}
 \frac{E}{2(1+\nu)} \left(\frac{\partial^2 u_x}{\partial x^2} + \frac{\partial^2 u_x}{\partial y^2} \right) + \frac{E}{2(1+\nu)(1-2\nu)} \left(\frac{\partial^2 u_x}{\partial x^2} + \frac{\partial^2 u_y}{\partial x \partial y} \right) + \rho \cdot f_x &= \rho \frac{\partial^2 u_x}{\partial t^2} \\
 \frac{E}{2(1+\nu)} \left(\frac{\partial^2 u_y}{\partial x^2} + \frac{\partial^2 u_y}{\partial y^2} \right) + \frac{E}{2(1+\nu)(1-2\nu)} \left(\frac{\partial^2 u_x}{\partial x \partial y} + \frac{\partial^2 u_y}{\partial y^2} \right) + \rho \cdot f_y &= \rho \frac{\partial^2 u_y}{\partial t^2}
 \end{aligned} \tag{2}$$

To assess this inversion algorithm we generated a displacement field $u = [u_x, u_y]$ using the 2D FE heart model undergoing a distributed load (i.e. body force) $f = [f_x, f_y]$ as described earlier. The force reconstruction algorithm was based on finite difference approximation. The spatial partial derivatives in equation (2) were computed using the displacement field at the nodes of a finite difference grid approximating the tissue geometry (Figure 1b). The grid was isotropic (i.e. $\Delta x = \Delta y$) in order to simplify the following finite difference approximation of the partial derivatives:

$$\begin{aligned}\frac{\partial^2 u}{\partial x^2}(x, y) &= \frac{u(x+1, y) - 2u(x, y) + u(x-1, y)}{(\Delta x)^2} \\ \frac{\partial^2 u}{\partial y^2}(x, y) &= \frac{u(x, y+1) - 2u(x, y) + u(x, y-1)}{(\Delta y)^2} \\ \frac{\partial^2 u}{\partial x^2}(x, y) &= \frac{u(x+1, y+1) - u(x+1, y-1) - u(x-1, y+1) + u(x-1, y-1)}{4(\Delta x)(\Delta y)}\end{aligned}\quad (3)$$

Boundary conditions were required to compute the displacements at fictitious nodes around the marginal nodes of the geometry, which facilitated computing the partial derivatives of the displacement field for the boundary nodes. These boundary conditions were approximated based on the flexing theory of thin plates²⁶. When computing the nodal acceleration, we separated the time and space dependence of the displacement field, according to an algorithm previously employed in soft tissue modeling for breast elastography²⁷. Since the loading was modeled as a harmonic force function, we assumed the response (i.e. the nodal displacements) to behave similarly, i.e. to be a harmonic function with similar frequency, but with a possible phase shift to account for viscosity, as shown in equation (4). This formulation lead to the separation of the space and time dependence of the displacement field: the first term, $U(s)$, is only dependent on the spatial coordinates (i.e. x, y, z), while the exponential term accounts for the time dependence, as follows:

$$\begin{aligned}u(s, t) &= U(s) \cdot e^{j\omega t} \\ \partial_t^2 u(s, t) &= -U(s) \cdot \omega^2 \cdot e^{j\omega t}\end{aligned}\quad (4)$$

where $U(s)$ is a spatial variable representing the motion magnitude and ω is the angular frequency. The equations of motion written for each space coordinate lead to two distinct equations, governing the real and imaginary components, respectively. After solving for the real and imaginary force component corresponding to each spatial coordinate, the force intensity was determined by taking the magnitude of the complex value in equation (5):

$$\begin{aligned}\frac{E}{2(1+\nu)} \left(\frac{\partial^2 U^R_x}{\partial x^2} + \frac{\partial^2 U^R_x}{\partial y^2} \right) + \frac{E}{2(1+\nu)(1-2\nu)} \left(\frac{\partial^2 U^R_x}{\partial x^2} + \frac{\partial^2 U^R_y}{\partial x \partial y} \right) + \rho \cdot f^R_x &= -\rho \omega^2 U^R_x \\ \frac{E}{2(1+\nu)} \left(\frac{\partial^2 U^I_x}{\partial x^2} + \frac{\partial^2 U^I_x}{\partial y^2} \right) + \frac{E}{2(1+\nu)(1-2\nu)} \left(\frac{\partial^2 U^I_x}{\partial x^2} + \frac{\partial^2 U^I_y}{\partial x \partial y} \right) + \rho \cdot f^I_x &= -\rho \omega^2 U^I_x \\ \frac{E}{2(1+\nu)} \left(\frac{\partial^2 U^R_y}{\partial x^2} + \frac{\partial^2 U^R_y}{\partial y^2} \right) + \frac{E}{2(1+\nu)(1-2\nu)} \left(\frac{\partial^2 U^R_x}{\partial x \partial y} + \frac{\partial^2 U^R_y}{\partial y^2} \right) + \rho \cdot f^R_y &= -\rho \omega^2 U^R_y \\ \frac{E}{2(1+\nu)} \left(\frac{\partial^2 U^I_y}{\partial x^2} + \frac{\partial^2 U^I_y}{\partial y^2} \right) + \frac{E}{2(1+\nu)(1-2\nu)} \left(\frac{\partial^2 U^I_x}{\partial x \partial y} + \frac{\partial^2 U^I_y}{\partial y^2} \right) + \rho \cdot f^I_y &= -\rho \omega^2 U^I_y \\ U_x &= U^R_x + iU^I_x, U_y = U^R_y + iU^I_y, f_x = f^R_x + if^I_x, f_y = f^R_y + if^I_y\end{aligned}\quad (5)$$

3. RESULTS

As described above, first a direct problem was formulated in order to generate tissue displacement data, which was ultimately used as input for the inverse algorithm, to reconstruct the contraction force distribution. Several simulations were performed in order to present various scenarios of how myocardial activity could be modeled, and to determine and test the efficiency of the developed technique. For all these cases, the contraction forces were assumed to act along the radial direction of the ventricle (i.e. $f_y = 0$).

3.1 Simulation of uniformly distributed contractile activity

In this case, the contraction force distribution was modeled as a uniformly distributed body force (per unit mass), with a magnitude of 50 m/s^2 at a driving frequency of 1.2 Hz. Figure 2 illustrates the reconstructed body force distribution, as well as a surface plot of the reconstruction error. The error was expressed as the difference between the original and reconstructed force field, normalized by the original distribution. To test the reproducibility of these results, another simulation involving a uniform body force distribution was performed, with a magnitude of 10 m/s^2 and at a driving frequency of 2.4 Hz. Figure 3 includes a plot of the reconstructed force field and the reconstruction error. The efficiency of the reconstruction can also be assessed by visual inspection of the reconstructed force field. The force was uniformly distributed across the inner region of the tissue slice, with a few exceptions in areas located in the vicinity of the boundaries. The reconstruction error averaged 0-10% in the regions located at the interior of the geometry of interest, while around the boundary the contraction forces were approximately two times larger than the reference force.

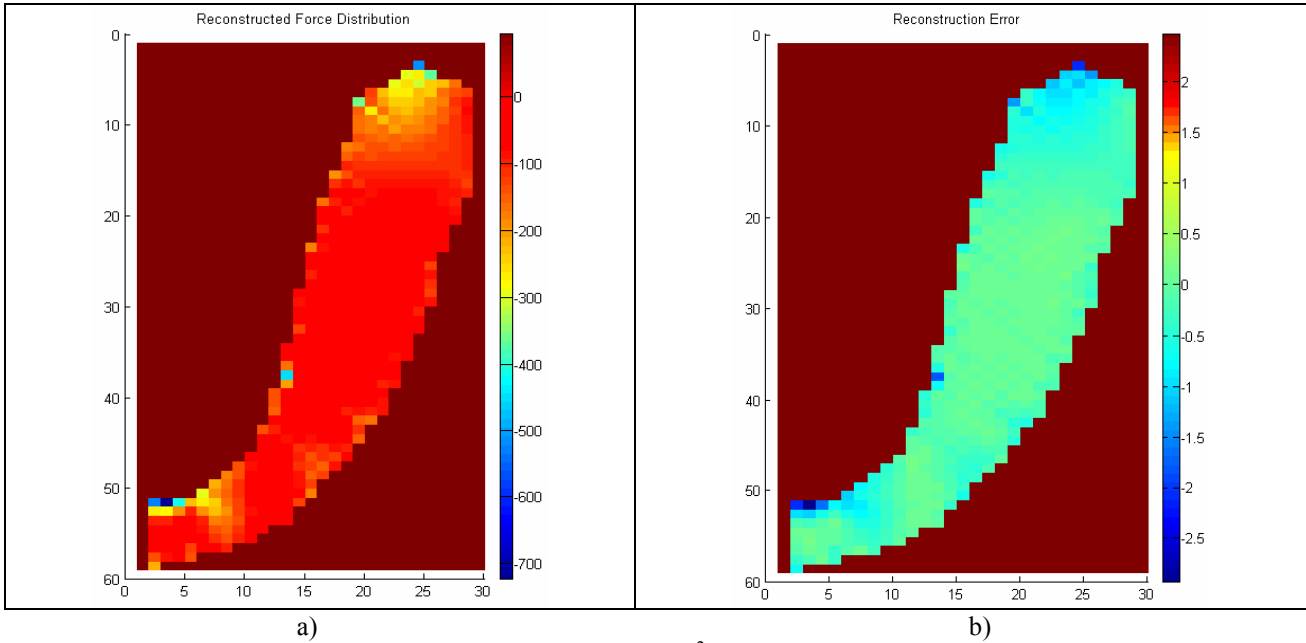


Figure 2: Uniformly distributed radial body force of magnitude 50 m/s^2 : a) Reconstructed force field, b) Reconstruction error

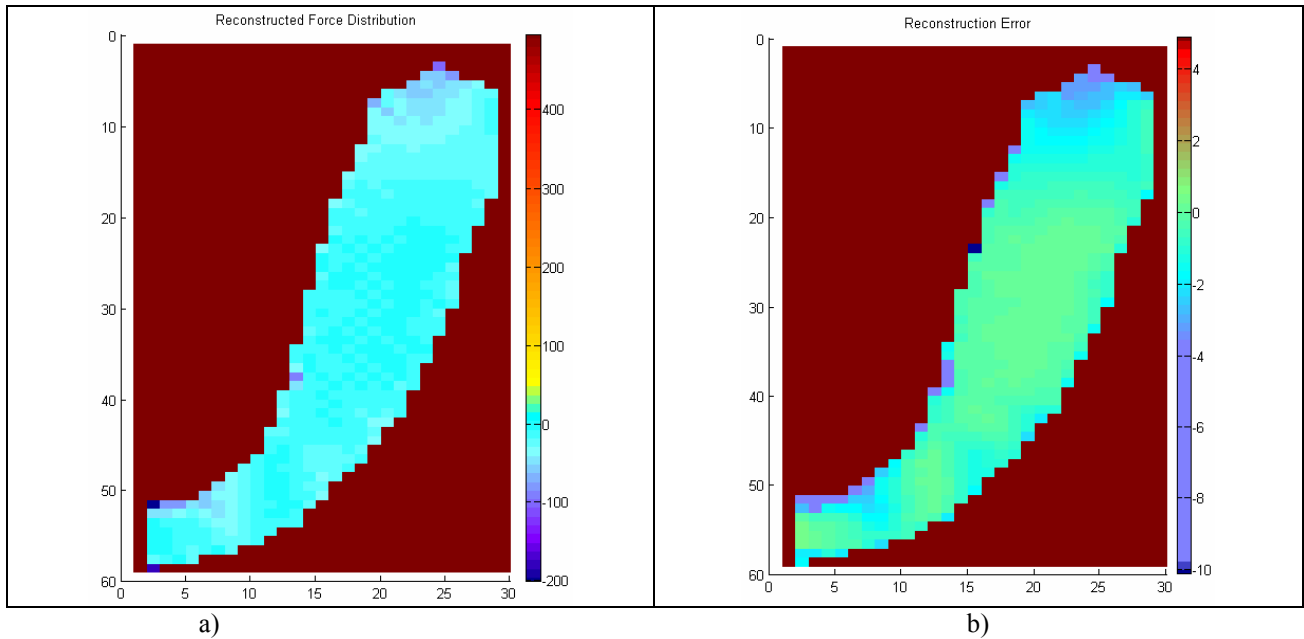


Figure 3: Uniformly distributed radial body force of magnitude 10 m/s^2 , and a driving frequency of 2.4 Hz: a) Reconstructed force field; b) Reconstruction error

3.2 Simulation of uniformly distributed contractile activity using superposition

The analysis was taken one step further by simulating another case of uniform contraction force distribution, which mimics a more realistic behaviour of the cardiac muscle. Since the cardiac activity may be approximated as a superposition of simple harmonics, the contractions were simulated as periodic, sinusoidal excitations of equal magnitude (25 m/s^2), but this time at two distinct driving frequencies: 1.2 and 2.4 Hz respectively. Based on the linearity of the system, the force distribution was computed by first inverting the displacements characteristic to each driving frequency, and ultimately superimposing the results. In practice, driving frequencies can be obtained using Fourier transforms. Figure 4 presents the reconstructed force distribution and the reconstruction error.

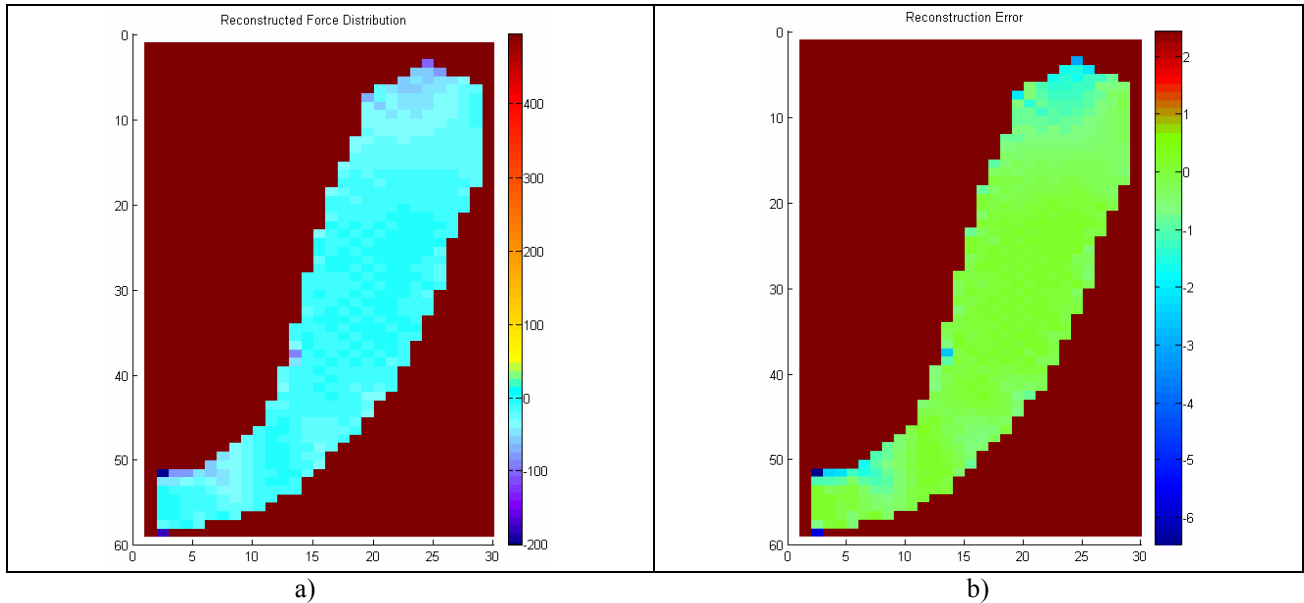


Figure 4: Superimposed, uniformly distributed radial body forces of magnitude 25 m/s^2 , at driving frequencies of 1.2 Hz and 2.4 Hz: a) Reconstructed force field; b) Reconstruction error

3.3 Simulation of diseased myocardial behaviour

Since the main purpose of this proposed technique is to assess the viability of cardiac tissue, while identifying infarcted regions, a simulation illustrating tissue necrosis was carried out. The tissue slice presented below contains a transmural infarct region located near the centre of the slice. Healthy, viable tissue was assumed to possess normal contractive capabilities, modeled using a body force distribution of 50 m/s^2 , while the infarcted region was modeled using a much lower body force magnitude of 10 m/s^2 . Figure 5 contains surface plots of the reconstructed force field and the error associated with the inversion, with the infarcted area outlined on the tissue slice.

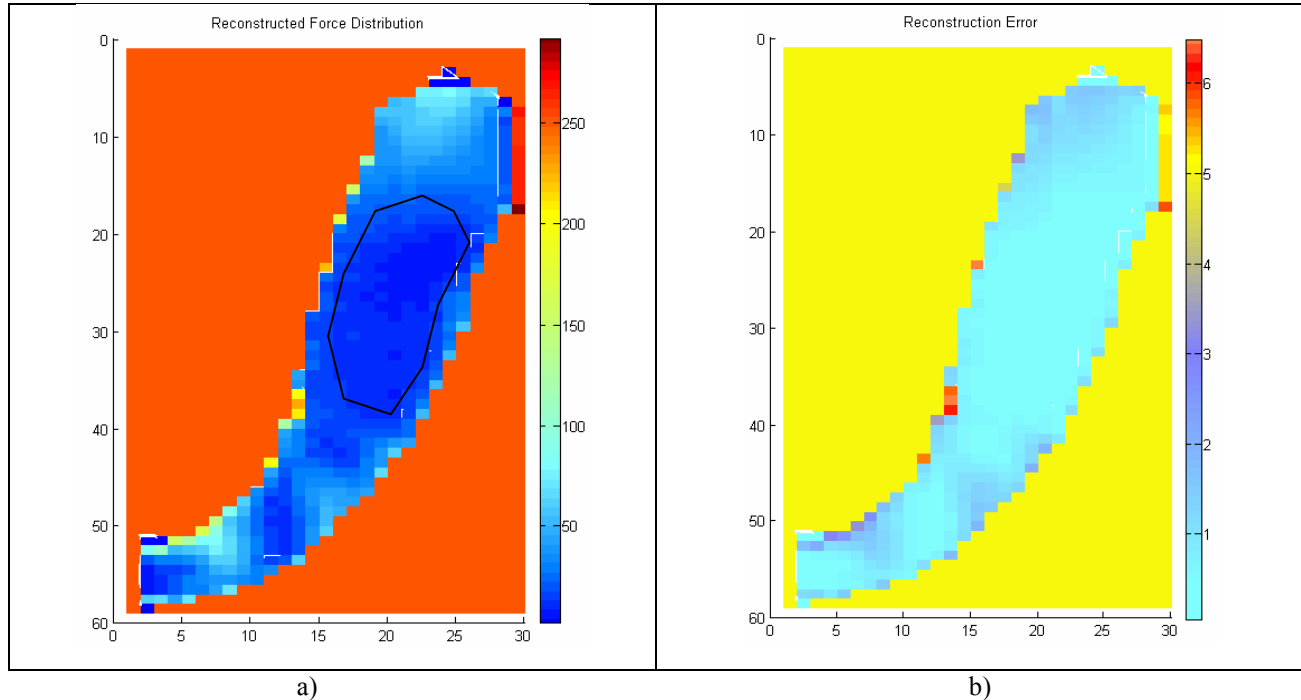


Figure 5: Simulation of diseased cardiac tissue containing a transmural infarct region located near the centre of the tissue slice (outlined by the contour): a) Reconstructed force field; b) Reconstruction error

4. DISCUSSIONS AND CONCLUSION

Current techniques for assessing tissue viability involving strain imaging and shortening index calculations are not only difficult to interpret, but also require a detailed database and history of previously diagnosed patients. This novel biomechanical technique is expected to enable clinicians to make a more accurate quantitative assessment regarding the cardiac tissue viability. It is expected to eliminate the degree of variability due to patient subjectivity introduced by the strain imaging methods, and display a distribution of contraction force across the myocardium, which can lead to a more accurate diagnosis.

Since no previous studies illustrate the modeling of myocardial contractions, we decided to first carry out a 2D analysis in order to demonstrate and test the possibility of myocardial contraction force reconstruction using a biomechanics approach. We used a previously explored two-dimensional axisymmetric ventricular geometry to model the heart muscle. We conducted several finite element analyses in order to simulate tissue displacement data, and used it to reconstruct the contraction force distribution associated with the response. Our analysis relied on assumptions based on cardiac functionality, physiology and structure, integrated within solid mechanics and tissue elasticity.

The accuracy of the reconstruction algorithm was assessed based on a comparison of the computed force distribution to the original one, and normalized with respect to the reference force field. For all cases, it was noticed that the reconstruction error was confined within the range of $\pm 10\%$, with the exception of small areas located in the vicinity of the slice boundaries. At these particular marginal locations, the reconstructed force field was contaminated by noise,

and the body force magnitudes were approximately two times larger than the real forces. In order to explain this phenomenon, a few speculations have been made. The reconstruction algorithm was based on an inverse problem solution, whose input consisted of tissue displacement data. For computational purposes, the nodal displacements obtained from the direct problem were overlaid on a finite difference grid, and computational kernels were used to evaluate the spatial derivatives of the nodal displacements. Taking into account the fact that for the boundary nodes the computational kernels operate on nodes external to the geometry of interest, fictitious nodal displacements were assigned for the nodes immediately exterior to the tissue geometry. Relationships between displacements in these fictitious nodes with those of the internal nodes were obtained based on the assumption of thin plate bending theory. One possibility to eliminate this error is to reformulate the boundary conditions used to assign these fictitious nodal displacements using more realistic assumptions. The forward FE problem used in our model can be further improved. The boundary conditions assumed for the tissue slice may not be the most appropriate. The endocardial and epicardial boundaries were modeled as free edges, while the basal edge adjacent to the mitral valve was constrained from motion, since it provides no useful contractive work. To improve the accuracy of the FE model in mimicking the actual myocardial deformation, a set of boundary conditions better simulating the tissue dynamics and cardiac physiology around the extremities could be implemented. Moreover, the displacements obtained under the prescribed loading conditions could be classified as large deformations, with strains exceeding 5%; however, the tissue was modeled as linear elastic, with a Young's modulus of 30 kPa at maximum deformation. Therefore, additional error was introduced due to the deformations extending beyond the range of applicability of linear elasticity. As such, to better model cardiac tissue contractions, we intend to account for a hyperelastic formulation of the inverse problem, accompanied by an optimization algorithm, which would enable us to improve the accuracy of the reconstruction algorithm.

In conclusion, we presented an algorithm for myocardial contraction force reconstruction from a two-dimensional model of cardiac tissue. The reconstruction algorithm was successfully applied to an axisymmetric ventricular geometry governed by isotropic linear elasticity, and the results were demonstrated to be consistent with the output data from a commercial FEA package. Therefore, these findings prove to be a step forward towards the development of a robust tool for assessing cardiac tissue viability, based on 3D contraction force reconstruction.

References

1. Heimdahl, A., Stoylen, A., Torp, H., and Skjaerpe, T., "Real-time strain rate imaging of the left ventricle by ultrasound," *J. Am. Soc. Echocardiogr.* **11**. 1013-1019 (1998).
2. Urheim, S., Edvardsen, T., Torp, H., Angelsen, B., and Smiseth, O. A., "Myocardial strain by Doppler echocardiography. Validation of a new method to quantify regional myocardial function," *Circulation* **102**. 1158-1164 (9-5-2000).
3. Stoylen, A., Heimdahl, A., Bjornstad, K., Torp, H. G., and Skjaerpe, T., "Strain Rate Imaging by Ultrasound in the Diagnosis of Regional Dysfunction of the Left Ventricle," *Echocardiography*. **16**. 321-329 (1999).
4. Wedeen, V. J., "Magnetic resonance imaging of myocardial kinematics. Technique to detect, localize, and quantify the strain rates of the active human myocardium," *Magn Reson. Med.* **27**. 52-67 (1992).
5. Bijnens, B., D'hooge, J., Schrooten, M., Pislaru, S., Pislaru, C., De, Man B., Nuyts, J., Suetens, P., Van de, Werf F., Sutherland, G. R., and Herregods, M. C., "Are changes in myocardial integrated backscatter restricted to the ischemic zone in acute induced ischemia? An in vivo animal study," *J. Am. Soc. Echocardiogr.* **13**. 306-315 (2000).
6. Sutherland, G. R., Stewart, M. J., Groundstroem, K. W., Moran, C. M., Fleming, A., Guell-Peris, F. J., Riemersma, R. A., Fenn, L. N., Fox, K. A., and McDicken, W. N., "Color Doppler myocardial imaging: a new technique for the assessment of myocardial function," *J. Am. Soc. Echocardiogr.* **7**. 441-458 (1994).
7. Palka, P., Lange, A., Fleming, A. D., Sutherland, G. R., Fenn, L. N., and McDicken, W. N., "Doppler tissue imaging: myocardial wall motion velocities in normal subjects," *J. Am. Soc. Echocardiogr.* **8**. 659-668 (1995).
8. Voigt, J. U., Arnold, M. F., Karlsson, M., Hubbert, L., Kukulski, T., Hatle, L., and Sutherland, G. R., "Assessment of regional longitudinal myocardial strain rate derived from doppler myocardial imaging indexes in normal and infarcted myocardium," *J. Am. Soc. Echocardiogr.* **13**. 588-598 (2000).
9. Castillo, E., Lima, J. A., and Bluemke, D. A., "Regional myocardial function: advances in MR imaging and analysis," *Radiographics* **23 Spec No.** S127-S140 (2003).
10. Picano, E., Lattanzi, F., Orlandini, A., Marini, C., and L'Abbate, A., "Stress echocardiography and the human factor: the importance of being expert," *J. Am. Coll. Cardiol.* **17**. 666-669 (3-1-1991).

11. Nagel, E., Lehmkuhl, H. B., Bocksch, W., Klein, C., Vogel, U., Frantz, E., Ellmer, A., Dreyse, S., and Fleck, E., "Noninvasive diagnosis of ischemia-induced wall motion abnormalities with the use of high-dose dobutamine stress MRI: comparison with dobutamine stress echocardiography," *Circulation* **99**. 763-770 (2-16-1999).
12. Delepine, S., Furber, A. P., Beygui, F., Prunier, F., Balzer, P., Le Jeune, J. J., and Geslin, P., "3-D MRI assessment of regional left ventricular systolic wall stress in patients with reperfused MI," *Am. J. Physiol Heart Circ. Physiol* **284**. H1190-H1197 (2003).
13. BURTON, A. C., "The importance of the shape and size of the heart," *Am. Heart J.* **54**. 801-810 (1957).
14. Balzer, P., Furber, A., Cavaro-Menard, C., Croue, A., Tadei, A., Geslin, P., Jallet, P., and Le Jeune, J. J., "Simultaneous and correlated detection of endocardial and epicardial borders on short-axis MR images for the measurement of left ventricular mass," *Radiographics* **18**. 1009-1018 (1998).
15. Furber, A., Balzer, P., Cavaro-Menard, C., Croue, A., Da, Costa E., Lethimonnier, F., Geslin, P., Tadei, A., Jallet, P., and Le Jeune, J. J., "Experimental validation of an automated edge-detection method for a simultaneous determination of the endocardial and epicardial borders in short-axis cardiac MR images: application in normal volunteers," *J. Magn Reson. Imaging* **8**. 1006-1014 (1998).
16. Gotte, M. J., van Rossum, A. C., Twisk, J. W. R., Kuijjer, J. P. A., Marcus, J. T., and Visser, C. A., "Quantification of regional contractile function after infarction: strain analysis superior to wall thickening analysis in discriminating infarct from remote myocardium," *J. Am. Coll. Cardiol.* **37**. 808-817 (3-1-2001).
17. Moore, C. C., McVeigh, E. R., and Zerhouni, E. A., "Quantitative tagged magnetic resonance imaging of the normal human left ventricle," *Top. Magn Reson. Imaging* **11**. 359-371 (2000).
18. Moore, C. C., Lugo-Olivieri, C. H., McVeigh, E. R., and Zerhouni, E. A., "Three-dimensional systolic strain patterns in the normal human left ventricle: characterization with tagged MR imaging," *Radiology* **214**. 453-466 (2000).
19. Axel, L., Goncalves, R. C., and Bloomgarden, D., "Regional heart wall motion: two-dimensional analysis and functional imaging with MR imaging," *Radiology* **183**. 745-750 (1992).
20. Zerhouni, E. A., Parish, D. M., Rogers, W. J., Yang, A., and Shapiro, E. P., "Human heart: tagging with MR imaging--a method for noninvasive assessment of myocardial motion," *Radiology* **169**. 59-63 (1988).
21. McVeigh, E. R., "MRI of myocardial function: motion tracking techniques," *Magn Reson. Imaging* **14**. 137-150 (1996).
22. Aelen, F. W., Arts, T., Sanders, D. G., Thelissen, G. R., Prinzen, F. W., and Reneman, R. S., "Kinematic analysis of left ventricular deformation in myocardial infarction using magnetic resonance cardiac tagging," *Int. J. Card Imaging* **15**. 241-251 (1999).
23. J.D.Humphrey, "Cardiovascular Solid Mechanics: Cells, Tissues and Organs," Springer - Verlag, (2002).
24. Declerck, J., Denney, T. S., Ozturk, C., O'Dell, W., and McVeigh, E. R., "Left ventricular motion reconstruction from planar tagged MR images: a comparison," *Phys. Med. Biol.* **45**. 1611-1632 (2000).
25. Guccione, J. M., Costa, K. D., and McCulloch, A. D., "Finite element stress analysis of left ventricular mechanics in the beating dog heart," *J. Biomech.* **28**. 1167-1177 (1995).
26. Ugural, A. C. Fenster S. K., "Advanced Strength and Applied Elasticity, Fourth Edition," Prentice Hall, (2003).
27. Sinkus, R., Lorenzen, J., Schrader, D., Lorenzen, M., Dargatz, M., and Holz, D., "High-resolution tensor MR elastography for breast tumour detection," *Phys. Med. Biol.* **45**. 1649-1664 (2000).